Planetary and Space Science 59 (2011) 788–797

Contents lists available at ScienceDirect

Planetary and Space Science

journal homepage: www.elsevier.com/locate/pss

Structured ionospheric outflow during the Cassini T55–T59 Titan flybys

N.J.T. Edberg [a,*], K. Ågren [a], J.-E. Wahlund [a], M.W. Morooka [a], D.J. Andrews [b], S.W.H. Cowley [b], A. Wellbrock [c], A.J. Coates [c], C. Bertucci [d], M.K. Dougherty [e]

[a] Swedish Institute of Space Physics, Box 537, 75121 Uppsala, Sweden
[b] Department of Physics & Astronomy, University of Leicester, Leicester LE1 7RH, UK
[c] Mullard Space Science Laboratory, University College London, Holmbury St Mary, Dorking RH5 6NT, UK
[d] Institute for Astronomy and Space Physics, Ciudad Universiteria, Buenos-Aires, Argentina
[e] Space and Atmospheric Physics Group, The Blackett Laboratory, Imperial College London, Prince Consort Road, London SW7 2BW, UK

ARTICLE INFO

Article history:
Received 3 December 2010
Received in revised form
11 March 2011
Accepted 12 March 2011
Available online 21 March 2011

Keywords:
Cassini
Titan
Atmospheric escape
Ionosphere

ABSTRACT

During the final three of the five consecutive and similar Cassini Titan flybys T55–T59 we observe a region characterized by high plasma densities (electron densities of 1–8 cm^{-3}) in the tail/nightside of Titan. This region is observed progressively farther downtail from pass to pass and is interpreted as a plume of ionospheric plasma escaping Titan, which appears steady in both location and time. The ions in this plasma plume are moving in the direction away from Titan and are a mixture of both light and heavy ions with composition revealing that their origin are in Titan's ionosphere, while the electrons are more isotropically distributed. Magnetic field measurements indicate the presence of a current sheet at the inner edge of this region. We discuss the mechanisms behind this outflow, and suggest that it could be caused by ambipolar diffusion, magnetic moment pumping or dispersive Alfvén waves.
© 2011 Elsevier Ltd. All rights reserved.

1. Introduction

All atmospheres in the solar system are slowly but continuously being eroded and lost into space. This has been observed through satellite measurements at Mars, Venus as well as at Titan (e.g., Lundin et al., 1989; Barabash et al., 2007; Wahlund et al., 2005). The rate of this atmospheric loss and the physical mechanisms that control it have been studied extensively. The loss rate at Mars and Venus have been measured to be of the order of 10^{24}–10^{25} particles per second and initial estimates at Titan are of the same orders of magnitude (Wahlund et al., 2005; Modolo et al., 2007). For the case of unmagnetized bodies the ionospheric plasma is being scavenged by the external flowing plasma and is transported away down the induced magnetospheric tail.

In this paper we report on a set of observations from Cassini at Titan, which show that the escape of ionospheric plasma from Titan can be very structured in location and that it indeed is a continuous process.

The early Voyager 1 measurements in 1982 showed that Titan had enough of an atmosphere that could be ionized such that an appreciable ionosphere could form around the moon, as was detected through radio occultation measurements (Bird et al., 1997). Prior to the observational evidence of the existence of an ionosphere it had been shown that an induced magnetosphere was formed around the moon as it interacted with the co-rotating plasma of Saturn (Ness et al., 1982; Neubauer et al., 1984).

After Cassini arrived at the Saturn system in 2004 and through the multitude of passes by Titan, knowledge of Titan's plasma environment has grown significantly. Backes et al. (2005) presented magnetic field measurements from the first Titan flyby (TA) which showed that Titan did not possess a strong intrinsic magnetic field. Hence Saturn's plasma interacts directly with the ionosphere of the moon. This interaction ideally leads to a characteristic pileup of Saturn's magnetic field around Titan (Bertucci et al., 2009) and the formation of a magnetospheric tail with a dual-lobe structure downstream of Titan (Neubauer et al., 2006). Using data from the first two passes by Titan Wahlund et al. (2005) presented measurements of the cold plasma environment of the moon. Saturn's dynamic plasma environment was shown to affect the structure of Titan's plasma environment and initial atmospheric escape rates of $\sim 10^{25}$ s^{-1} were presented. Categorization of each flyby by ambient plasma properties (Rymer et al., 2009) and by ambient magnetic field properties (Simon et al., 2010) have shown that Titan is truly situated in a dynamic space environment.

Photoionization was shown to be the main ionospheric ionizing process (Ågren et al., 2009), but impacting magnetospheric particles from Saturn also contribute, especially to the production of the night side ionosphere (e.g., Cravens et al., 2005, 2008, 2009; Ågren et al., 2007; Galand et al., 2010). Plasma transport from the dayside to the nightside has also been suggested as a possible contributor to the ionosphere (Cui et al., 2009, 2010). The

* Corresponding author.
E-mail address: ne@irfu.se (N.J.T. Edberg).

0032-0633/$ - see front matter © 2011 Elsevier Ltd. All rights reserved.
doi:10.1016/j.pss.2011.03.007

structure of the ionosphere was studied by Kliore et al. (2008) through radio occultation measurements from Cassini and was found to be variable and with a main peak at an altitude of 1200 km. Larger statistical studies using Langmuir probe measurements confirm this (Edberg et al., 2010a), and have also shown that it varies with solar illumination angle and upstream magnetospheric conditions (Ågren et al., 2009). Ågren et al. (in press) presented the first detections of ionospheric currents and associated electric fields in Titan's ionosphere during three Cassini passes, indicating that electrodynamic processes are occurring.

Cassini measurements have shown the presence of complex chemistry in the ionosphere. Cravens et al. (2006) showed that the most abundant species in the ionosphere are $HCNH^+$ and $C_2H_5^+$. A wealth of additional species, mostly organic molecules, are also present (Waite et al., 2005). The detection of heavy (>100 amu) ions (positive and negative) adds to the chemical complexity in the upper atmosphere (Coates et al., 2007a, 2009; Waite et al., 2007; Wahlund et al., 2009; Vuitton et al., 2009; Crary et al., 2009).

In addition to new observational findings there have been many attempts to model the ionosphere and its interaction with the Saturnian plasma. Pre-Cassini, (Ip, 1990; Keller et al., 1992, 1998; Galand et al., 1999) made early attempts to model Titan's ionospheric structure, composition and variability. Post-arrival of Cassini, several models of Titan's ionosphere have been produced (e.g., Cravens et al., 2005, 2009; Vuitton et al., 2007; Robertson et al., 2009). Furthermore, there have been numerous attempts to try to model and simulate the ionosphere's interaction with the co-rotating plasma of Saturn. Ma et al. (2006, 2007, 2009) used a MHD code to simulate this interaction while Sillanpää et al. (2006, 2007), Simon et al. (2006, 2007), and Modolo et al. (2007) used hybrid simulation codes. Despite detailed differences, all models are fairly good at reproducing the general features of Titan's global plasma environment and its interaction with Saturn's co-rotating plasma.

In this paper we will study the structure of the outflow of this ionospheric plasma from Titan. Using five similar Titan flybys, i.e. T55–T59, which systematically and gradually change the flyby trajectory from pass to pass, we are able to study where plasma escape occurs in the tail region of Titan. We will also provide some suggestions for which mechanisms control the ionospheric plasma escape.

This paper is structured as follows. In Section 2 we introduce the instruments used, while in Section 3 we describe the orbit geometry of the Titan flybys. In Section 4 we present the observational findings, and in Section 5 we summarize and discuss the results.

2. Instrumentation

The Cassini spacecraft carries three instruments which have been used in this study and which will be described in this section.

2.1. Radio and plasma wave science

The Radio and Plasma Wave Science (RPWS) investigation includes three orthogonal search coil magnetic antennas, three orthogonal electric field antennas and a Langmuir probe (LP) (Gurnett et al., 2004; Wahlund et al., 2005) out of which we use the LP and electric field antennas.

The Langmuir probe consists of a spherical shell, with a diameter of 5 cm, fastened to a stub, which is situated on a 1.5 m boom mounted on the spacecraft bus. It is a versatile instrument with different operating modes. Here, we will only use measurements from when the probe is in the so-called 'sweep' mode. In this mode the voltage which is fed to the probe sweeps from -4 to $+4$ V in 512 steps (or from -32 to $+32$ V in 1024 steps), and the current, drawn from electrons and ions in the plasma, is collected. Normally, the probe sweeps in the shorter voltage range when the closest approach of a Titan flyby reaches below 1400 km. A sweep is carried out every 24 s. From the characteristic current–voltage curve the electron density, n_e; the electron temperature, T_e; and the floating potential of the probe, U_{float} can be determined. The floating potential measured at the probe also gives a measure of the spacecraft potential $U_{S/C}$ through the relation

$$U_{S/C}-U_{float}=cU_{S/C}e^{-d_{LP}/\lambda_D}, \tag{1}$$

where $d_{LP}=1.5$ m is the distance from the probe to the spacecraft bus, λ_D is the Debye length of the ambient plasma, and $c\approx 5/6$ is a constant. The electron density and temperature estimates are based on a theoretical fit to the current–voltage curve which takes into account up to three electron populations, and is based on a three-electron and one drifting ion component orbit motion limited (OML) theory (Mott-Smith and Langmuir, 1926; Medicus, 1962; Whipple, 1965; Fahleson et al., 1974). One electron population consists of the spacecraft photoelectrons, while the others are the ionospheric electrons, which are of central interest here. The electron current sampled by the probe in the OML approximation for one electron population and positive voltages is

$$I_e=I_{e0}(1-\chi_e), \tag{2}$$

where

$$I_{e0}=A_{LP}n_e q_e\sqrt{\frac{k_B T_e}{2\pi m_e}} \tag{3}$$

is the random current, A_{LP} is the probe area, and

$$\chi_e=\frac{q_e(U_{bias}+U_1)}{k_B T_e}, \tag{4}$$

where k_B is Boltzmann's constant, m_e the electron mass, q_e the electron charge, U_{bias} the applied voltage, and U_1 the characteristic potential of the electron population (equal to the floating potential U_{float} for the photoelectron population). When the plasma density falls below ~ 5 cm^{-3}, the floating potential can be used as a proxy for the electron density. Morooka et al. (2009) showed that the floating potential was related to the electron density, as measured by the electron spectrometer instrument (ELS), through an exponential function. The average ion mass m_i, the ion density n_i, and the ion bulk speed v_i can also be determined under certain conditions, but as those parameters will not be used in this paper, we will not describe those considerations here.

In a dense plasma (above ~ 1 cm^{-3}) the RPWS electric antennas can also detect electric field emissions at the upper hybrid resonance frequency

$$f_{UH}=\sqrt{f_p^2+f_c^2}, \tag{5}$$

where $f_p=1/2\pi\sqrt{n_e q_e^2/m_e\varepsilon_0}$ is the electron plasma frequency, $f_c=q_e B/m_e$ the electron cyclotron frequency, ε_0 the permittivity of free space, and B the magnetic field strength. Since $f_p\gg f_c$ in the situations discussed here, it follows that $f_{UH}\approx f_p=8980\sqrt{n_e}$, which means that from observations of the upper hybrid frequency the local electron density can be calculated independently, and can be compared to the density measured by the LP.

2.2. Cassini particle spectrometer

The ELS instrument, which is part of the Cassini Particle Spectrometer (CAPS) package, measures electrons in the energy range 0.6–28 keV with an energy resolution $\Delta E/E=0.17$, a field of view of 5.2° × 160° (eight elevation sectors of 20° each) and a time resolution of 2 s (Young et al., 2004). In this paper we present the ELS measurements as differential energy flux (DEF) averaged over all anodes. The CAPS package also includes an ion mass spectrometer (IMS) from which we have retrieved some preliminary information on ion composition to support the results in this paper.

2.3. Magnetometer

The Cassini Magnetic field experiment (MAG) consists of a fluxgate sensor (FGM) which is mounted on a boom 5.5 m away from the spacecraft bus. It is capable of measuring vector magnetic fields at a rate of 2 Hz (Dougherty et al., 2004). In this paper we will use 1 s averaged FGM vector magnetic field measurements.

2.4. Coordinate system

The magnetic field vector components, as well as Cassini's position throughout the paper, are presented in the Titan interaction coordinate system (TIIS) where the *x* axis is directed along the co-rotation direction of Saturn's magnetospheric plasma, the *y* axis is directed toward Saturn and the *z* axis completes the right handed system.

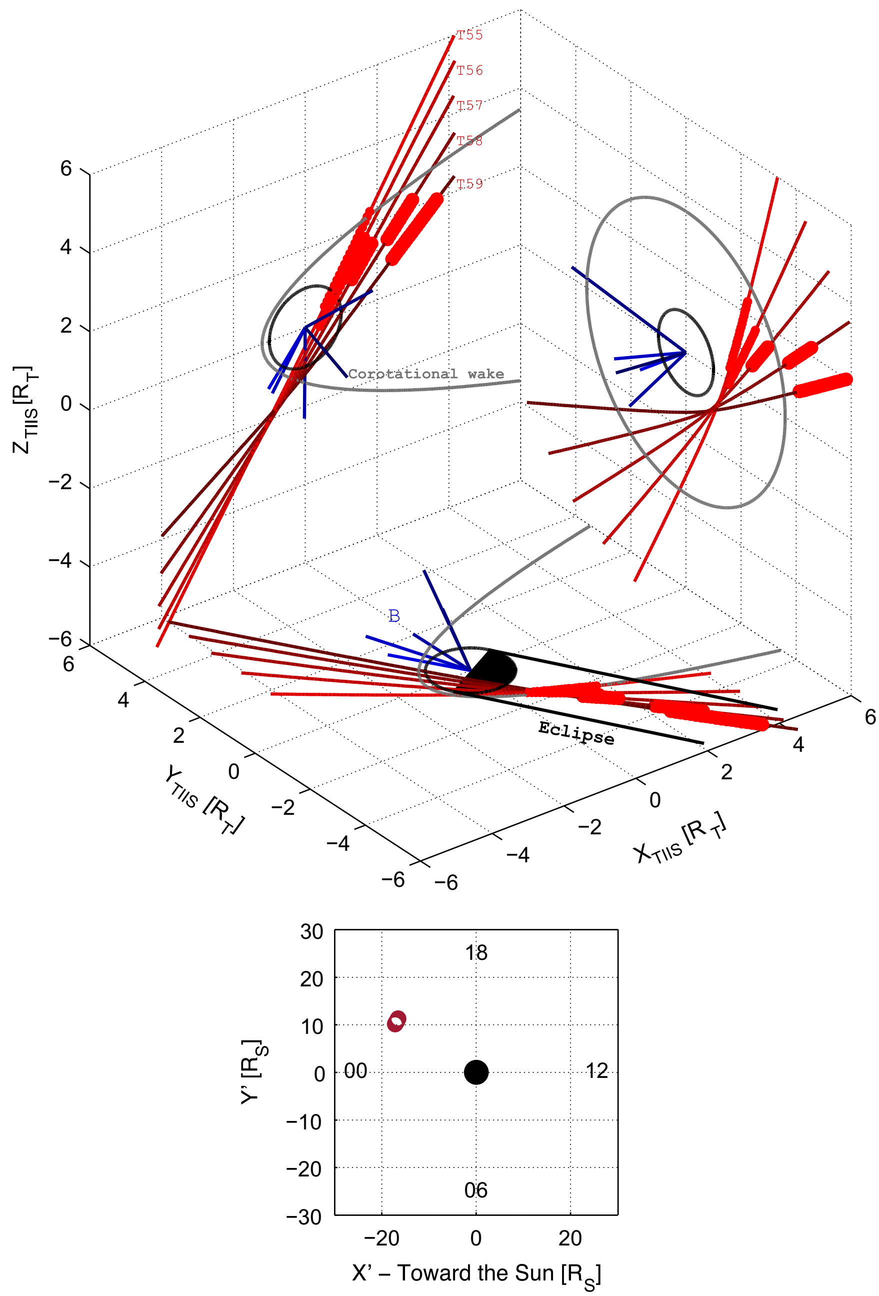

Fig. 1. (Top) The flyby configuration in three planes in the TIIS system. The red thin lines show the trajectory of Cassini for the T55–T59 flybys while the thick red lines on top of the T55 and T56 tracks indicate the region of an extended ionosphere. The thick red lines on top of the T57, T58 and T59 tracks indicate the interval when the density plume is observed (see Figs. 4–6). For orientation purposes the gray lines indicate the shape of an approximate induced magnetospheric boundary and the black lines indicate the eclipse region, i.e. the region in shadow of Titan. The blue lines show the average components of the magnetic field for each flyby. The components are (b_x, b_y, b_z)=(−1.03, 1.67, −1.21), (−0.92, 2.61, −1.36), (−0.02, 2.01, −2.32), (1.88, 4.15, 0.28) and (1.17, 2.54, −1.68) nT. (Bottom) The position of Titan relative to Saturn during the T55–T59 flybys shown as red circles. All flybys took place at around 22 h Saturn local time. (For interpretation of the references to color in this figure legend, the reader is referred to the web version of this article.)

3. Flyby geometry

To date, more than 70 Titan flybys have been carried out by Cassini. They have taken place at a large range of Saturn local times and have mapped a large fraction of the near-Titan space such that most flyby configurations differ from the others. The T55–T59 flybys are, however, unique in the sense that their flyby geometries are similar from pass to pass, except for a gradual decrease in the latitude of closest approach and for a gradual change in inclination. Hence, the T55–T59 flybys enable systematic studies of Titan's plasma environment. The T60 flyby also followed the same trend, but no RPWS, ELS or MAG data were gathered during that pass so it is omitted from this study.

The upper panel of Fig. 1 shows the trajectory of Cassini during the T55–T59 flybys projected onto the *x*–*y*, *x*–*z*, and *y*–*z* planes, in the TIIS coordinate system, while the lower panel shows the location of Titan relative to Saturn during these flybys. All five flybys occurred at 22 h Saturn local time such that the ideal direction of the co-rotational flow and the anti-sunward direction are separated by 60°, meaning that the eclipse region, i.e. the region shadowed by Titan, and the co-rotation wake are far from coincident. Cassini approached Titan from the wake and nightside during each pass and had its closest approaches at latitudes $-22°$ (T55), $-32°$ (T56), $-42°$ (T57), $-52°$ (T58), and $-62°$ (T59). The T55 flyby had the highest inclination while the T59 flyby had the lowest.

In Fig. 1 the average magnetic field vectors for each flyby are also shown projected onto the three planes, which will be discussed further below. The averages are calculated over 30 min prior to each flyby. On top of the spacecraft trajectories are three intervals highlighted by thick red lines. These intervals mark the position where plasma escaping from Titan was observed. These observations, which are the prime focus of this paper, will be described in detail in the following section.

4. Observations

Figs. 2–6 show time series of combined RPWS, MAG, and ELS data during the five Titan flybys T55–T59. The top four panels in each plot show RPWS measurements of the cold plasma, while the lowest two panels show vector magnetic field data and ELS-measured DEF spectrograms. Each figure shows exactly 2 h of data centered at closest approach in order to simplify the comparison between the five flybys.

During the T55 flyby (Fig. 2) Cassini is in Saturn's magnetosphere from the beginning of the time series at 20:30 UT until 21:00 UT, when the electron density starts to increase, indicating an entry into the nightside exo-ionosphere of Titan at an altitude of $\sim$7000 km. The density increases gradually until 21:20 UT when the ionosphere proper is entered. From 21:10 to 21:20 UT Cassini is in Titan's

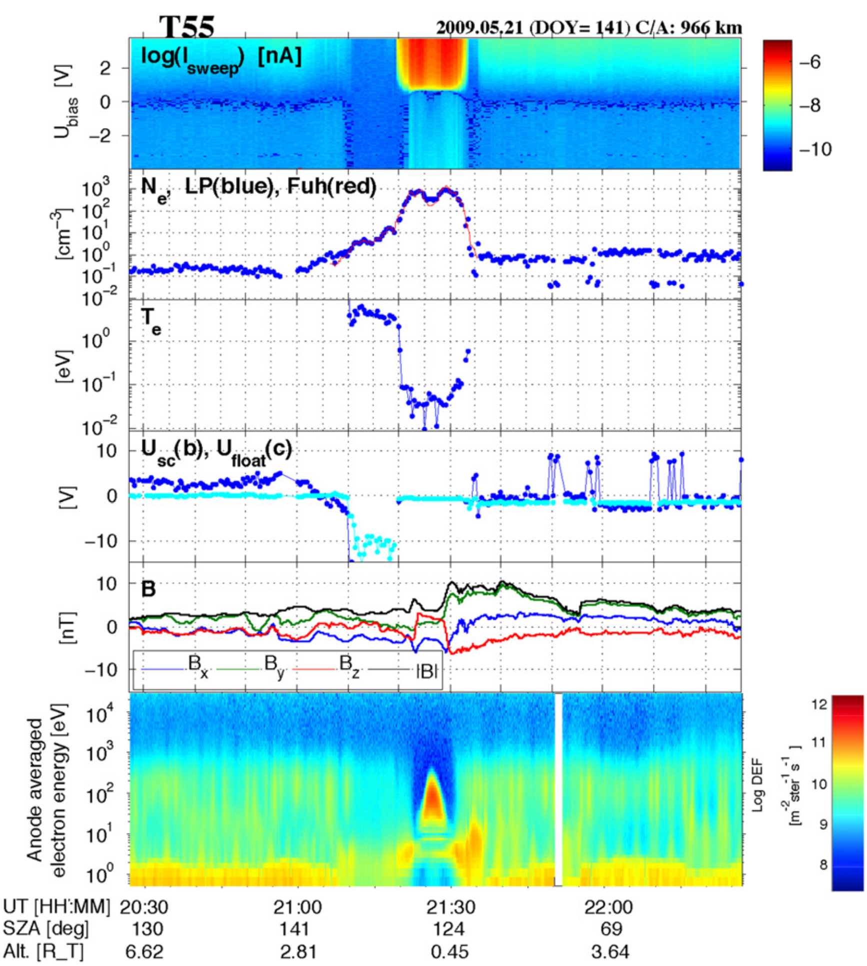

Fig. 2. Cassini RPWS, MAG, and ELS data from the T55 flyby shown as a time series. The panels show from top to bottom: the LP voltage–current characteristics, LP measured electron density (blue) together with the density derived from the upper hybrid frequency line as measured by the RPWS electric antennas (red), LP electron temperature, LP floating potential (cyan) and LP spacecraft potential (blue), MAG vector magnetic fields in TIIS coordinates, and an ELS electron spectrogram. (For interpretation of the references to color in this figure legend, the reader is referred to the web version of this article.)

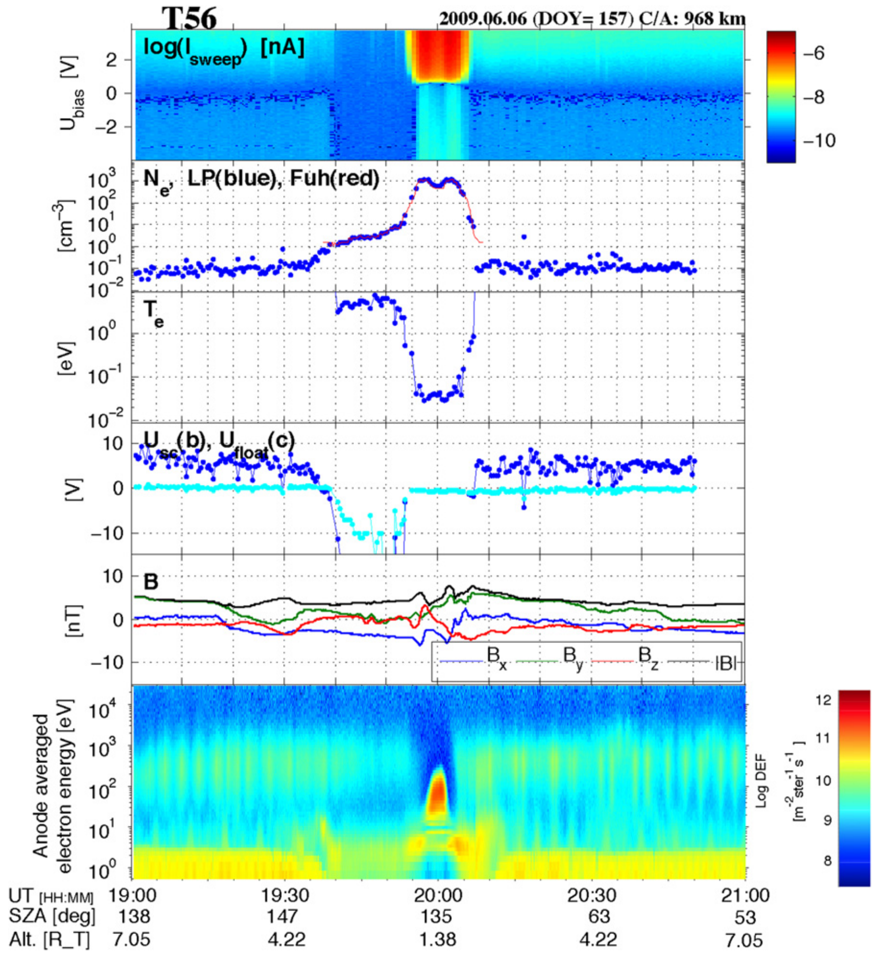

Fig. 3. Same as for Fig. 2 except for T56.

shadow. Surprisingly perhaps, the density does not decrease in this region, which is a first indication of that ionospheric plasma from Titan is escaping through the wake/night region. The temperature increases significantly in this region indicating the presence of heating mechanisms, while the spacecraft potential becomes very negative due to lack of a balancing photoelectron current from the spacecraft. The ionosphere proper is sampled for 15 min, from 21:20 until 21:35 UT, during which time the ionospheric peak altitude of ~ 1100 km is crossed twice. When the electron density increases in the ionosphere, the electron temperature decreases as described by Edberg et al. (2010a). The spacecraft potential stays negative at a constant value of -0.7 V during the ionospheric pass, and the low energy electrons are then not visible in the ELS electron spectrogram. The significant increase in flux values between energies 10 and 500 eV in the ELS data at around closest approach (21:26 UT) are detections of negative ions as discussed for the T55–T59 flybys by Coates et al. (2010). After 21:32 UT a sharp drop in the density is observed as Cassini quickly exits Titan's ionosphere and enters the outer plasma environment of the moon. The ionospheric plasma is very asymmetrically distributed around Titan, with an extended ionospheric tail on the nightside. This is indicated by a thick red line on top of the trajectory line in Fig. 1. Cassini leaves Titan's ionosphere on the ram side of Titan where a magnetic pile-up region is observed and the magnetic field gradually decreases until 21:55 UT.

When the density is less than $\sim 5\ \mathrm{cm}^{-3}$, i.e. before 21:10 UT and in the interval after 21:35 UT, the density is obtained through the LP density proxy (see Section 2). When the density proxy is used it is implied that the electron temperature cannot be readily estimated from the sweep data. Note also that it is not possible to obtain the density from the LP sweep data in the eclipse region due to the strong shift in spacecraft potential. Instead, the voltage–current fit is calibrated to the density obtained through the upper hybrid resonance frequency (Eq. (5)) such that the electron temperature and spacecraft potential can be estimated from the LP sweeps. The electron temperature values and the spacecraft potential values are therefore more uncertain in the eclipse region. The ELS measured low energy electrons do, however, disappear when the eclipse region is entered indicating that the spacecraft potential indeed goes strongly negative.

The data gathered during the following flyby, T56 (Fig. 3), show the same general trend in the data as in the T55 pass. Cassini approaches Titan from the wake side, goes into a slightly longer eclipse than during the previous pass since the trajectory has changed somewhat and is slightly less inclined, before traversing the ionosphere and finally leaving the Titan environment on the ram side. Again, ionospheric plasma is observed to be extended downstream on the wake side in the interval 19:35–19:55 UT which is indicated by a red line in Fig. 1. During the following three Titan passes, T57, T58 and T59, the observations follow the same trend, but with crucial differences.

The difference during the T57–T59 passes (Figs. 4–6), that is of particular interest in this paper, is that an isolated high density plasma region, consisting of detached cold ionospheric plasma, is observed in the tail region of Titan. This is seen progressively farther back in the tail during each flyby. For T57, an enhanced density region with a peak density of $\sim 8\ \mathrm{cm}^{-3}$ is observed in the RPWS data in the interval 18:05–18:15 UT, in the altitude range 4500–7500 km. The RPWS measurements are supported by the

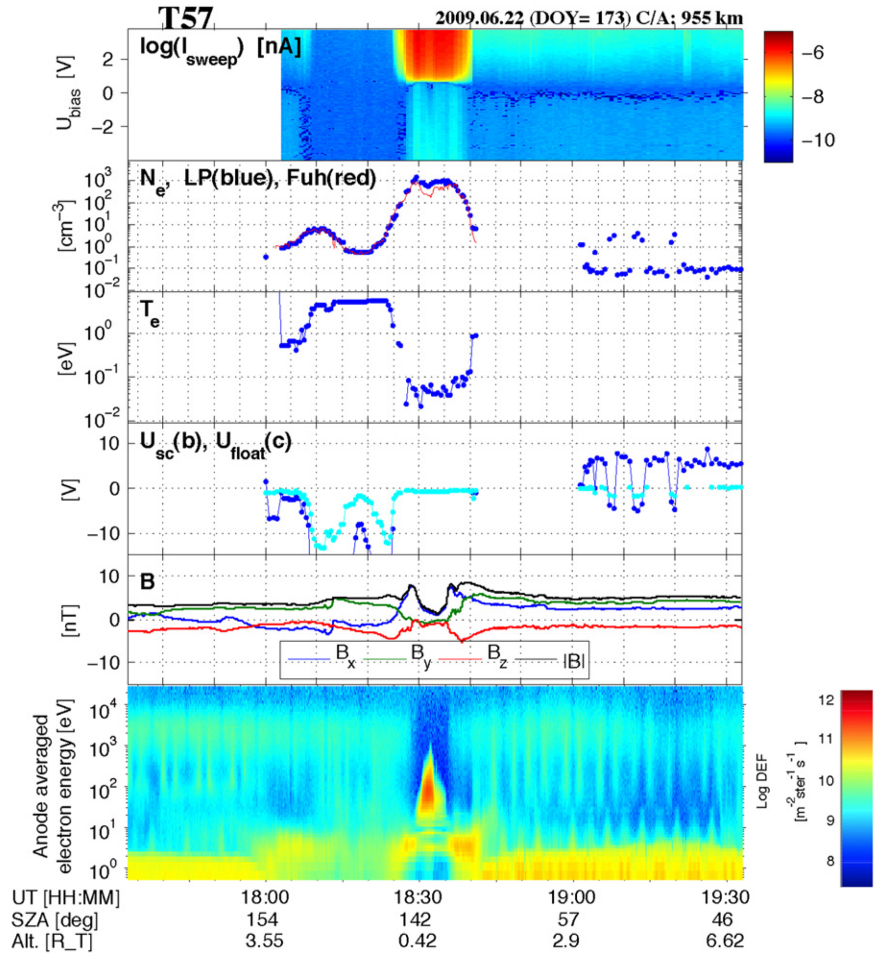

Fig. 4. Same as for Fig. 2 except for T57.

ELS electron measurements, which show a coincident increase in the DEF during the same interval for energies below 10 eV. The MAG measurements show that the magnetic field undergoes a change in direction at the end of this interval, at ~18:12 UT, indicating the presence of a current sheet. The position of this density increase interval is marked by a thick red line on top of the T57 trajectory line in the geometry plot of Fig. 1.

During the following pass, T58, a similar density increase is observed in the LP density data at 16:20–16:32 UT, in the altitude range 8000–13000 km. This time the density increase is observed even farther back in the tail than during the previous pass as can be seen in Fig. 1. The ELS flux measurements do not indicate any increased low energy fluxes, as during the previous pass. The MAG measurements do, however, reveal a major rotation of the magnetic field, again at the inner edge of the density region, which again indicates the presence of a current sheet.

Finally, during the T59 flyby, the density increase is observed for a third consecutive pass in the interval 14:40–15:00 UT in Fig. 6. These observations take place in the altitude range 9000–15 000 km. The ELS low energy fluxes are now again coincidentally increasing, while the MAG measurements show only relatively weak magnetic field fluctuations.

5. Discussion and summary

In Fig. 7 we show the five altitude profiles of the measured electron densities during T55–T59. During the final three of the five consecutive and similar flybys, the high density ($\sim 1-8\ cm^{-3}$) plasma region observed downstream of Titan is marked by shaded regions. This tail-like structure is observed progressively farther away from Titan from pass to pass. We interpret these observations as evidence that cold ionospheric plasma is escaping Titan and is being transported downstream in a spatially limited escape plume. CAPS/IMS ion measurements (not shown) indicate that the ions in this region are coming from Titan, most likely in a magnetic flux tube connected to Titan's ionosphere, while the electrons seem to be isotropically distributed. The very structured way in which the density increase is observed indicates that Cassini is traversing the same quasi-stationary high density region during all flybys but at different distances from Titan. It is less likely that the density increases are sporadically detached plasma clouds, which happen to be situated at the location of Cassini during three consecutive flybys. Preliminary ion composition measurements from CAPS/IMS reveal that the ions in this high-density region are both light and heavy species with a composition indicating that their origin are in Titan's ionosphere (*Ronan Modolo, private communication*). Observations of cold ionospheric plasma in the far tail region were also reported from the T9 flyby of Titan (Coates et al., 2007b; Modolo et al., 2007; Szego et al., 2007; Wei et al., 2007), but the observed morphology here differs from that.

It is also worth mentioning that high density plasma regions have been observed downstream of the other unmagnetized objects, Venus and Mars, but with some differences in appearance. At Venus, plasma 'clouds' have been observed as a regular phenomena in the nightside, (Brace et al., 1982; Brace and Kliore, 1991). These do not appear as a steady plume like the findings reported here but rather as sporadic events. Ong et al. (1991)

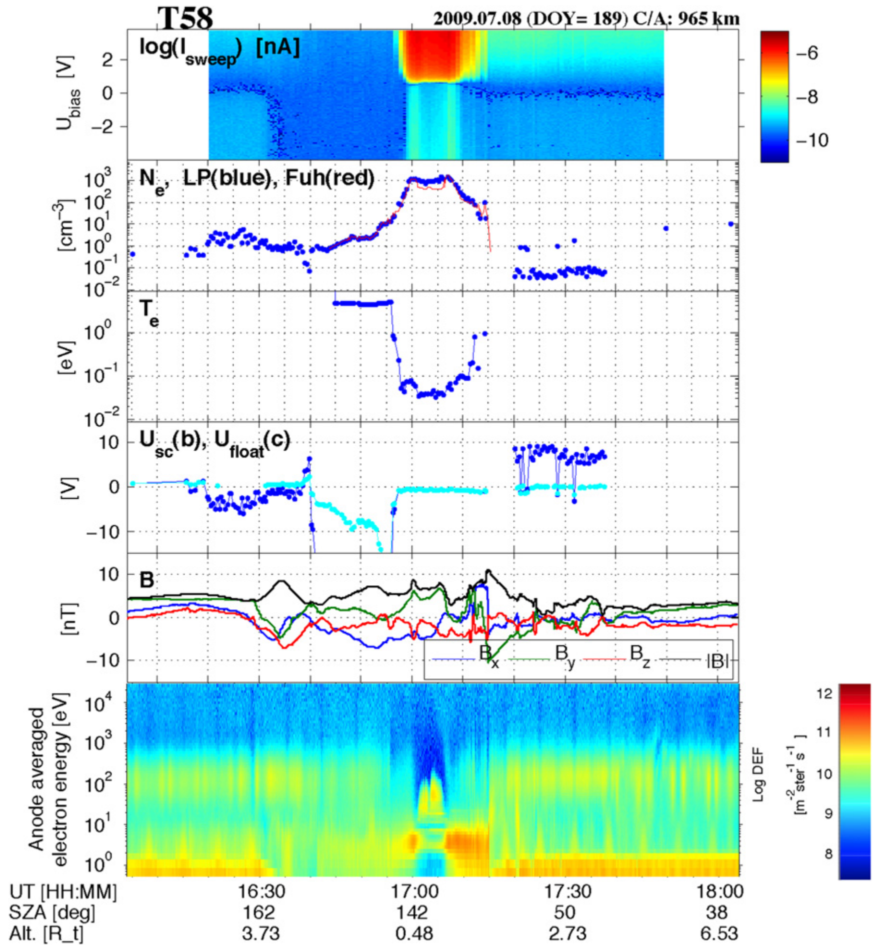

Fig. 5. Same as for Fig. 2 except for T58.

related the plasma 'clouds' to changes in the orientation of the interplanetary magnetic field, which drapes around the planet, during solar wind sector boundary crossings. That situation is not likely to be occurring here since Saturn's dipole field does not change polarity like the solar wind. At Mars, Brain et al. (2010) reported observations of intermittently escaping bulk ionospheric plasma. This bulk removal occurred when the streaming solar wind plasma stretched the Martian crustal magnetic field, which in turn dragged out ionospheric plasma. The stretched crustal magnetic field is then detached through magnetic reconnection. Titan does not posses strong crustal fields which could trigger this type of events. Sporadic increase in the loss of ionospheric plasma from Mars and Venus has also been associated with the impact of co-rotating interaction regions and coronal mass ejections on each planet (e.g., Luhmann et al., 2007, 2008; Dubinin et al., 2008; Edberg et al., 2010b; McEnulty et al., 2010). This could possibly be analogous to a general triggering mechanism for increased escape of Titan's ionosphere. Since the co-rotating plasma of Saturn also show great variation in plasma density it could act in a similar way as solar wind storms and sporadically enhance the ionospheric escape.

The structured escape plume is similar to the results from global 3D simulations by e.g., Sillanpää et al. (2006, 2007) and Modolo et al. (2007) with the difference that their observed main outflow is located on the Saturn-side of Titan (in the $+y$ region), while these observations occur on the anti-Saturn side. However, a minor region of high ionospheric plasma density can be seen on the anti-Saturn side in the simulations of Modolo et al. (2007). The outflow asymmetry in their models is dependent on the direction of the magnetic field **B** and the co-rotational flow direction $\mathbf{v}_{corot}$, which determines the direction of the convective electric field $\mathbf{E}_{conv} = -\mathbf{v}_{corot} \times \mathbf{B}$. An 'ideal' flow in the $+x$ direction and a magnetic field primarily in the $-z$ direction would give a convective electric field in the $-y$ direction. This is essentially how the model runs were set up and is similar to the situation during our observations, except that here there are strong x and y components of the magnetic field, as shown by the blue average magnetic field vectors in Fig. 1. Therefore, the structured outflow we report here does not seem to be governed by the convective electric field. During the T9 flyby, the incident flow direction, which also influences the direction of the convective electric field, was far from the 'ideal'. Strong fluctuations in the flow direction could possibly cause loss of plasma in a sporadic fashion through the build-up of surface instabilities at the ionosphere–magnetosphere interface. However, this would be unlikely to occur during three consecutive flybys. The ambient magnetic field is measured to be relatively steady during each flyby.

Fig. 8 displays a summarizing cartoon of three possible causes of the observations. One possible driver of the outflow is ambipolar diffusion, which adds a pressure gradient $-\nabla p$ to the fluid motion equation, and which is caused by electric fields set up partly by ionospheric photoelectrons, as was discussed for the similar observations during the T9 encounter (Coates et al., 2007b). Our observations take place close to, or within, the eclipse region. We speculate that since photoelectrons are produced in the sunlit region but not in the eclipse region it is possible that ambipolar electric fields, due to the charge separation, are set up and

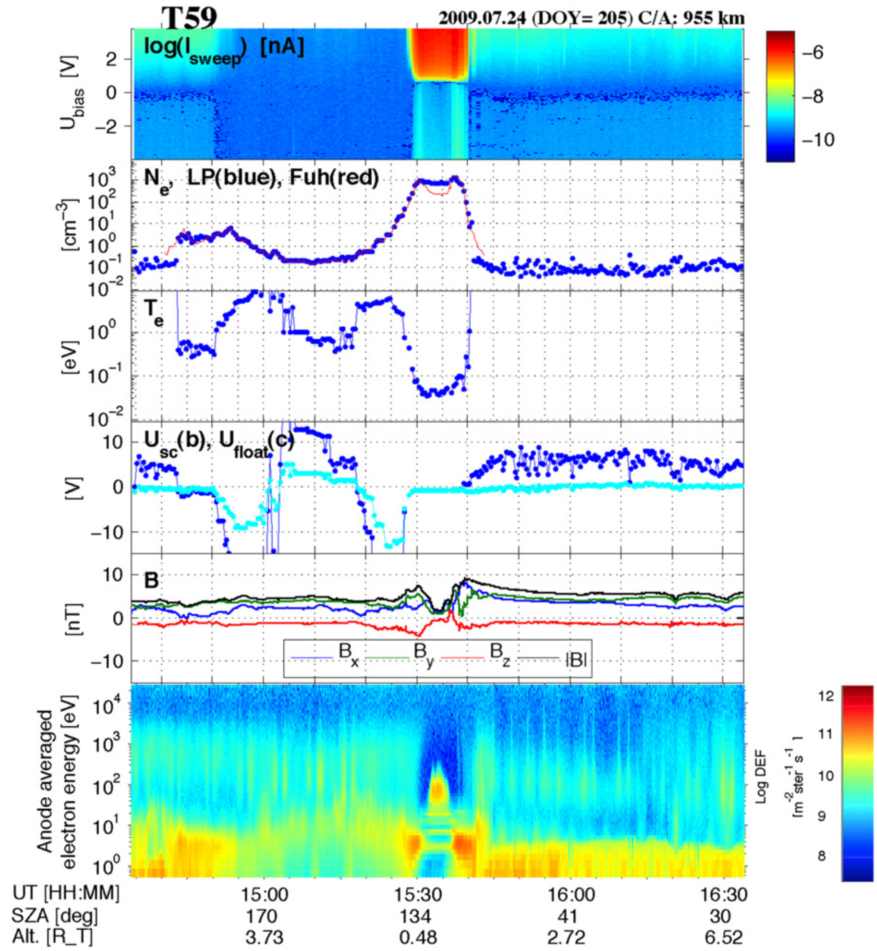

Fig. 6. Same as for Fig. 2 except for T59.

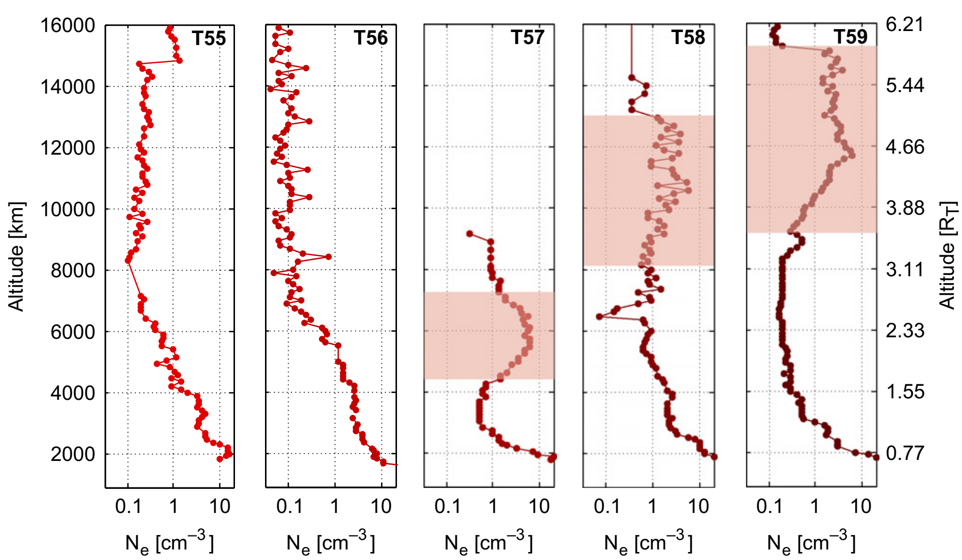

Fig. 7. Altitude profiles of the electron density measured during the inbound legs of the T55–T59 flybys. The observations of the electron plume are highlighted by the shaded regions.

accelerate ionospheric plasma away from Titan, like Earth's polar wind.

Magnetic moment pumping, which adds another gradient term, $-\mu\nabla_{\parallel}\mathbf{B}$, to the fluid motion equation, could be another mechanism behind the observed escape (e.g., Lundin and Hultqvist, 1989). The draped field lines in the induced magnetosphere around Titan have a gradient that goes from the tail to the ram side. The presence of this field strength gradient means that a force will act on the plasma and accelerate it in the tailward direction.

A third possible mechanism is dispersive Alfvén waves that are being generated in the exo-ionosphere of Titan, break down to broadband extremely low frequency (BB-ELF) waves and

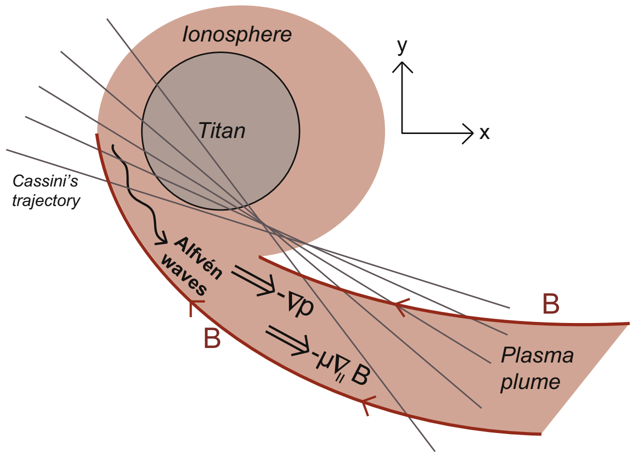

Fig. 8. A cartoon of the system showing three possible causes of the observed ionospheric escape.

accelerate ions in the tailward direction (e.g., Louarn et al., 1994; Wahlund et al., 1994; Knudsen et al., 1998). However, we do not observe any Alfvénic fluctuations in the data so if this would be the explanation then the waves would have to be generated closer to the ram side of the moon.

We cannot say for sure which mechanism that is responsible, but rather suggest that one of the above mentioned, or several of them combined, should be considered when trying to explain the observed structured atmospheric outflow.

Acknowledgments

N.J.T.E., K.Å. and J.W. acknowledge funding from the Swedish Research Council (VR). The Swedish National Space Board (SNSB) supports the RPWS/LP instrument onboard Cassini.

References

Ågren, K., Wahlund, J.-E., Modolo, R., Lummerzheim, D., Galand, M., Müller-Wodarg, I., Canu, P., Kurth, W.S., Cravens, T.E., Yelle, R.V., Waite Jr., J.H., Coates, A.J., Lewis, G.R., Young, D.T., Bertucci, C., Dougherty, M.K., 2007. On magnetospheric electron impact ionisation and dynamics in Titan's ram-side and polar ionosphere—a Cassini case study. Ann. Geophys. 25, 2359–2369.

Ågren, K., Wahlund, J.-E., Garnier, P., Modolo, R., Cui, J., Galand, M., Müller-Wodarg, I., 2009. On the ionospheric structure of Titan. Planet. Space. Sci. 57, 1821–1827. doi:10.1016/j.pss.2009.04.012.

Ågren, K., Andrews, D.J., Buchert, A.J., Coates, S.C., Cowley, S.W.H., Dougherty, M.K., Edberg, N.J.T., Garnier, P., Lewis, G.R., Modolo, R., Opgenoorth, H., Provan, G., Rosenqvist, L., Talboys, D.L., Wahlund, J.-E., Wellbrock, A., Detection of currents and associated electric fields in Titans ionosphere from Cassini data. J. Geophys. Res., in press. doi:10.1029/2010JA016100.

Backes, H., Neubauer, F.M., Dougherty, M.K., Achilleos, N., André, N., Arridge, C.S., Bertucci, C., Jones, G.H., Khurana, K.K., Russell, C.T., Wennmacher, A., 2005. Titan's magnetic field signature during the first Cassini encounter. Science 308, 992–995. doi:10.1126/science.1109763.

Barabash, S., Fedorov, A., Sauvaud, J.J., Lundin, R., Russell, C.T., Futaana, Y., Zhang, T.L., Andersson, H., Brinkfeldt, K., Grigoriev, A., Holmström, M., Yamauchi, M., Asamura, K., Baumjohann, W., Lammer, H., Coates, A.J., Kataria, D.O., Linder, D.R., Curtis, C.C., Hsieh, K.C., Sandel, B.R., Grande, M., Gunell, H., Koskinen, H.E.J., Kallio, E., Riihelä, P., Säles, T., Schmidt, W., Kozyra, J., Krupp, N., Fränz, M., Woch, J., Luhmann, J., McKenna-Lawlor, S., Mazelle, C., Thocaven, J., Orsini, S., Cerulli-Irelli, R., Mura, M., Milillo, M., Maggi, M., Roelof, E., Brandt, P., Szego, K., Winningham, J.D., Frahm, R.A., Scherrer, J., Sharber, J.R., Wurz, P., Bochsler, P., 2007. The loss of ions from Venus through the plasma wake. Nature 450, 650–653. doi:10.1038/nature06434.

Bertucci, C., Sinclair, B., Achilleos, N., Hunt, P., Dougherty, M.K., Arridge, C.S., 2009. The variability of Titan's magnetic environment. Planet. Space Sci. 57, 1813–1820. doi:10.1016/j.pss.2009.02.009.

Bird, M.K., Dutta-Roy, R., Asmar, S.W., Rebold, T.A., 1997. Detection of Titan's ionosphere from Voyager 1 radio occultation observations. Icarus 130, 426–436. doi:10.1006/icar.1997.5831.

Brace, L.H., Kliore, A.J., 1991. The structure of the Venus ionosphere. Space Sci. Rev. 55, 81–163. doi:10.1007/BF00177136.

Brace, L.H., Theis, R.F., Hoegy, W.R., 1982. Plasma clouds above the ionopause of Venus and their implications. Planet. Space. Sci. 30, 29–37. doi:10.1016/0032-0633(82)90069-1.

Brain, D.A., Baker, A.H., Briggs, J., Eastwood, J.P., Halekas, J.S., Phan, T., 2010. Episodic detachment of Martian crustal magnetic fields leading to bulk atmospheric plasma escape. Geophys. Res. Lett. 37, L14108. doi:10.1029/2010GL043916.

Coates, A.J., Crary, F.J., Lewis, G.R., Young, D.T., Waite, J.H., Sittler, E.C., 2007a. Discovery of heavy negative ions in Titan's ionosphere. Geophys. Res. Lett. 34, L22103. doi:10.1029/2007GL030978.

Coates, A.J., Crary, F.J., Young, D.T., Szego, K., Arridge, C.S., Bebesi, Z., Sittler, E.C., Hartle, R.E., Hill, T.W., 2007b. Ionospheric electrons in Titan's tail: plasma structure during the Cassini T9 encounter. Geophys. Res. Lett. 34, L24S05. doi:10.1029/2007GL030919.

Coates, A.J., Wellbrock, A., Lewis, G.R., Jones, G.H., Young, D.T., Crary, F.J., Waite, J.H., 2009. Heavy negative ions in Titan's ionosphere: altitude and latitude dependence. Planet. Space. Sci. 57, 1866–1871. doi:10.1016/j.pss.2009.05.009.

Coates, A.J., Wellbrock, A., Lewis, G.R., Jones, G.H., Young, D.T., Crary, F.J., Waite, J.H., Johnson, R.E., Hill, T.W., Sittler Jr., E.C., 2010. Negative ions at Titan and Enceladus: recent results. Faraday Discuss. 147, 293–305. doi::10.1039/C004700G.

Crary, F.J., Magee, B.A., Mandt, K., Waite, J.H., Westlake, J., Young, D.T., 2009. Heavy ions, temperatures and winds in Titan's ionosphere: Combined Cassini CAPS and INMS observations. Planet. Space. Sci. 57, 1847–1856. doi:10.1016/j.pss.2009.09.006.

Cravens, T.E., Robertson, I.P., Clark, J., Wahlund, J., Waite, J.H., Ledvina, S.A., Niemann, H.B., Yelle, R.V., Kasprzak, W.T., Luhmann, J.G., McNutt, R.L., Ip, W., De La Haye, V., Müller-Wodarg, I., Young, D.T., Coates, A.J., 2005. Titan's ionosphere: model comparisons with Cassini Ta data. Geophys. Res. Lett. 32, L12108. doi:10.1029/2005GL023249.

Cravens, T.E., Robertson, I.P., Waite, J.H., Yelle, R.V., Kasprzak, W.T., Keller, C.N., Ledvina, S.A., Niemann, H.B., Luhmann, J.G., McNutt, R.L., Ip, W., De La Haye, V., Mueller-Wodarg, I., Wahlund, J., Anicich, V.G., Vuitton, V., 2006. Composition of Titan's ionosphere. Geophys. Res. Lett. 33, L7105. doi:10.1029/2005GL025575.

Cravens, T.E., Robertson, I.P., Ledvina, S.A., Mitchell, D., Krimigis, S.M., Waite, J.H., 2008. Energetic ion precipitation at Titan. Geophys. Res. Lett. 35, L03103. doi:10.1029/2007GL032451.

Cravens, T.E., Robertson, I.P., Waite, J.H., Yelle, R.V., Vuitton, V., Coates, A.J., Wahlund, J., Agren, K., Richard, M.S., de La Haye, V., Wellbrock, A., Neubauer, F.M., 2009. Model-data comparisons for Titan's nightside ionosphere. Icarus 199, 174–188. doi:10.1016/j.icarus.2008.09.005.

Cui, J., Galand, M., Yelle, R.V., Vuitton, V., Wahlund, J.-E., Lavvas, P.P., Müller-Wodarg, I.C.F., Cravens, T.E., Kasprzak, W.T., Waite Jr., J.H., 2009. Diurnal variations of Titan's ionosphere. J. Geophys. Res. 114, A06310. doi:10.1029/2009JA014228.

Cui, J., Galand, M., Yelle, R.V., Wahlund, J., Ågren, K., Waite, J.H., Dougherty, M.K., 2010. Ion transport in Titan's upper atmosphere. J. Geophys. Res. 115(A14) (A06314). doi:10.1029/2009JA014563.

Dougherty, M.K., Kellock, S., Southwood, D.J., Balogh, A., Smith, E.J., Tsurutani, B.T., Gerlach, B., Glassmeier, K., Gleim, F., Russell, C.T., Erdos, G., Neubauer, F.M., Cowley, S.W.H., 2004. The Cassini magnetic field investigation. Space Sci. Rev. 114, 331–383. doi:10.1007/s11214-004-1432-2.

Dubinin, E., Modolo, R., Fränz, M., Woch, J., Akalin, F., Gurnett, D., Lundin, R., Barabash, S., Plaut, J.J., Picardi, G., 2008. Structure and dynamics of the solar wind/ionosphere interface on Mars. MEX-ASPERA-3 and MEX-MARSIS observations. Geophys. Res. Lett. 35, L11103. doi:10.1029/2008GL033730.

Edberg, N.J.T., Wahlund, J.-E., Ågren, K., Morooka, M.W., Modolo, R., Bertucci, C., Dougherty, M.K., 2010a. Electron density and temperature measurements in the cold plasma environment of Titan—implications for atmospheric escape. Geophys. Res. Lett. 37, L20105. doi:10.1029/2010GL044544.

Edberg, N.J.T., Nilsson, H., Williams, A.O., Lester, M., Milan, S.E., Cowley, S.W.H., Fränz, M., Barabash, S., Futaana, Y., 2010b. Pumping out the atmosphere of Mars through solar wind pressure pulses. Geophys. Res. Lett. 37, L03107. doi:10.1029/2009GL041814.

Fahleson, U., Fälthammar, C., Pedersen, A., 1974. Ionospheric temperature and density measurements by means of spherical double probes. Planet. Space. Sci. 22, 41–66. doi:10.1016/0032-0633(74)90122-6.

Galand, M., Lilensten, J., Toublanc, D., Maurice, S., 1999. The ionosphere of Titan: ideal diurnal and nocturnal cases. Icarus 140, 92–105. doi:10.1006/icar.1999.6113.

Galand, M., Yelle, R., Cui, J., Wahlund, J., Vuitton, V., Wellbrock, A., Coates, A., 2010. Ionization sources in Titan's deep ionosphere. J. Geophys. Res. 115 (A14), A07312. doi:10.1029/2009JA015100.

Gurnett, D.A., Kurth, W.S., Kirchner, D.L., Hospodarsky, G.B., Averkamp, T.F., Zarka, P., Lecacheux, A., Manning, R., Roux, A., Canu, P., Cornilleau-Wehrlin, N., Galopeau, P., Meyer, A., Boström, R., Gustafsson, G., Wahlund, J.-E., Åhlen, L., Rucker, H.O., Ladreiter, H.P., Macher, W., Woolliscroft, L.J.C., Alleyne, H., Kaiser, M.L., Desch, M.D., Farrell, W.M., Harvey, C.C., Louarn, P., Kellogg, P.J., Goetz, K., Pedersen, A., 2004. The cassini radio and plasma wave investigation. Space Sci. Rev. 114, 395–463. doi:10.1007/s11214-004-1434-0.

Ip, W., 1990. Titan's upper ionosphere. Astrophys. J. 362, 354–363. doi:10.1086/169271.

Keller, C.N., Cravens, T.E., Gan, L., 1992. A model of the ionosphere of Titan. J. Geophys. Res. 97 (A8), 12,117–12,235. doi:10.1029/92JA00231.

Keller, C.N., Anicich, V.G., Cravens, T.E., 1998. Model of Titan's ionosphere with detailed hydrocarbon ion chemistry. Planet. Space. Sci. 46, 1157–1174.
Kliore, A.J., Nagy, A.F., Marouf, E.A., French, R.G., Flasar, F.M., Rappaport, N.J., Anabttawi, A., Asmar, S.W., Kahann, D.S., Barbinis, E., Goltz, G.L., Fleischman, D.U., Rochblatt, D.J., 2008. First results from the Cassini radio occultations of the Titan ionosphere. J. Geophys. Res. 113, A09317. doi:10.1029/2007JA012965.
Knudsen, D.J., Clemmons, J.H., Wahlund, J., 1998. Correlation between core ion energization, suprathermal electron bursts, and broadband ELF plasma waves. J. Geophys. Res. 103, 4171–4186. doi:10.1029/97JA00696.
Louarn, P., Wahlund, J.E., Chust, T., de Feraudy, H., Roux, A., Holback, B., Dovner, P.O., Eriksson, A.I., Holmgren, G., 1994. Observation of kinetic Alfvén waves by the Freja spacecraft. Geophys. Res. Lett. 21, 1847–1850. doi:10.1029/94GL00882.
Luhmann, J.G., Kasprzak, W.T., Russell, C.T., 2007. Space weather at Venus and its potential consequences for atmosphere evolution. J. Geophys. Res. 112 (E11), E04S10. doi:10.1029/2006JE002820.
Luhmann, J.G., Fedorov, A., Barabash, S., Carlsson, E., Futaana, Y., Zhang, T.L., Russell, C.T., Lyon, J.G., Ledvina, S.A., Brain, D.A., 2008. Venus Express observations of atmospheric oxygen escape during the passage of several coronal mass ejections. J. Geophys. Res. 113 (E12), E00B04. doi:10.1029/2008JE003092.
Lundin, R., Hultqvist, B., 1989. Ionospheric plasma escape by high-altitude electric fields—magnetic moment 'pumping'. J. Geophys. Res. 94, 6665–6680. doi:10.1029/JA094iA06p06665.
Lundin, R., Borg, H., Hultqvist, B., Zakharov, A., Pellinen, R., 1989. First measurements of the ionospheric plasma escape from Mars. Nature 341, 609–612. doi:10.1038/341609a0.
Ma, Y., Nagy, A.F., Cravens, T.E., Sokolov, I.V., Hansen, K.C., Wahlund, J., Crary, F.J., Coates, A.J., Dougherty, M.K., 2006. Comparisons between MHD model calculations and observations of Cassini flybys of Titan. J. Geophys. Res. 111, A05207. doi:10.1029/2005JA011481.
Ma, Y., Nagy, A.F., Toth, G., Cravens, T.E., Russell, C.T., Gombosi, T.I., Wahlund, J., Crary, F.J., Coates, A.J., Bertucci, C.L., Neubauer, F.M., 2007. 3D global multispecies Hall-MHD simulation of the Cassini T9 flyby. Geophys. Res. Lett. 34, L24S10. doi:10.1029/2007GL031627.
Ma, Y.J., Russell, C.T., Nagy, A.F., Toth, G., Bertucci, C., Dougherty, M.K., Neubauer, F.M., Wellbrock, A., Coates, A.J., Garnier, P., Wahlund, J., Cravens, T.E., Crary, F.J., 2009. Time-dependent global MHD simulations of Cassini T32 flyby: From magnetosphere to magnetosheath. J. Geophys. Res. 114, A03204. doi:10.1029/2008JA013676.
McEnulty, T.R., Luhmann, J.G., de Pater, I., Brain, D.A., Fedorov, A., Zhang, T.L., Dubinin, E., 2010. Interplanetary coronal mass ejection influence on high energy pick-up ions at Venus. Planet. Space. Sci. 58, 1784–1791. doi:10.1016/j.pss.2010.07.019.
Medicus, G., 1962. Spherical Langmuir probe in drifting and accelerated Maxwellian distribution. J. Appl. Phys. 33, 3094–3100. doi:10.1063/1.1728574.
Modolo, R., Chanteur, G.M., Wahlund, J.-E., Canu, P., Kurth, W.S., Gurnett, D., Matthews, A.P., Bertucci, C., 2007. Plasma environment in the wake of Titan from hybrid simulation: a case study. Geophys. Res. Lett. 34, L24S04. doi:10.1029/2007GL030489.
Morooka, M.W., Modolo, R., Wahlund, J., André, M., Eriksson, A.I., Persoon, A.M., Gurnett, D.A., Kurth, W.S., Coates, A.J., Lewis, G.R., Khurana, K.K., Dougherty, M., 2009. The electron density of Saturn's magnetosphere. Ann. Geophys. 27, 2971–2991.
Mott-Smith, H.M., Langmuir, I., 1926. The theory of collectors in gaseous discharges. Phys. Rev. 28, 727–763. doi:10.1103/PhysRev.28.727.
Ness, N.F., Acuna, M.H., Behannon, K.W., 1982. The induced magnetosphere of Titan. J. Geophys. Res. 87, 1369–1381. doi:10.1029/JA087iA03p01369.
Neubauer, F.M., Gurnett, D.A., Scudder, J.D., Hartle, R.E., 1984. In: Titan's Magnetospheric Interaction. University of Arizona Press, Tucson, AZ, pp. 760–787 (Chapter 3).
Neubauer, F.M., Backes, H., Dougherty, M.K., Wennmacher, A., Russell, C.T., Coates, A., Young, D., Achilleos, N., André, N., Arridge, C.S., Bertucci, C., Jones, G.H., Khurana, K.K., Knetter, T., Law, A., Lewis, G.R., Saur, J., 2006. Titan's near magnetotail from magnetic field and electron plasma observations and modeling: Cassini flybys Ta, Tb, T3. J. Geophys. Res. 111 (A10), A10,220. doi:10.1029/2006JA011676.
Ong, M., Luhmann, J.G., Russell, C.T., Strangeway, R.J., Brace, L.H., 1991. Venus ionospheric 'clouds' - Relationship to the magnetosheath field geometry. J. Geophys. Res. 96, 11,133–11,144. doi:10.1029/91JA01100.
Robertson, I.P., Cravens, T.E., Waite, J.H., Yelle, R.V., Vuitton, V., Coates, A.J., Wahlund, J.E., Ågren, K., Mandt, K., Magee, B., Richard, M.S., Fattig, E., 2009. Structure of Titan's ionosphere: model comparisons with Cassini data. Planet. Space Sci. 57, 1834–1846. doi:10.1016/j.pss.2009.07.011.
Rymer, A.M., Smith, H.T., Wellbrock, A., Coates, A.J., Young, D.T., 2009. Discrete classification and electron energy spectra of Titan's varied magnetospheric environment. Geophys. Res. Lett. 36, L15109. doi:10.1029/2009GL039427.
Sillanpää, I., Kallio, E., Janhunen, P., Schmidt, W., Mursula, K., Vilppola, J., Tanskanen, P., 2006. Hybrid simulation study of ion escape at Titan for different orbital positions. Adv. Space Res. 38, 799–805. doi:10.1016/j.asr.2006.01.005.
Sillanpää, I., Kallio, E., Jarvinen, R., Janhunen, P., 2007. Oxygen ions at Titan's exobase in a Voyager 1-type interaction from a hybrid simulation. J. Geophys. Res. 112, A12205. doi:10.1029/2007JA012348.
Simon, S., Bößwetter, A., Bagdonat, T., Motschmann, U., Glassmeier, K., 2006. Plasma environment of Titan: a 3-D hybrid simulation study. Ann. Geophys. 24, 1113–1135.
Simon, S., Bößwetter, A., Bagdonat, T., Motschmann, U., Schuele, J., 2007. Three-dimensional multispecies hybrid simulation of Titan's highly variable plasma environment. Ann. Geophys. 25, 117–144.
Simon, S., Wennmacher, A., Neubauer, F.M., Bertucci, C.L., Kriegel, H., Saur, J., Russell, C.T., Dougherty, M.K., 2010. Titan's highly dynamic magnetic environment: a systematic survey of Cassini magnetometer observations from flybys TA-T62. Planet. Space. Sci. 58, 1230–1251. doi:10.1016/j.pss.2010.04.021.
Szego, K., Bebesi, Z., Bertucci, C., Coates, A.J., Crary, F., Erdos, G., Hartle, R., Sittler, E.C., Young, D.T., 2007. Charged particle environment of Titan during the T9 flyby. Geophys. Res. Lett. 34, L24S03. doi:10.1029/2007GL030677.
Vuitton, V., Yelle, R.V., McEwan, M.J., 2007. Ion chemistry and N-containing molecules in Titan's upper atmosphere. Icarus 191, 722–742. doi:10.1016/j.icarus.2007.06.023.
Vuitton, V., Lavvas, P., Yelle, R.V., Galand, M., Wellbrock, A., Lewis, G.R., Coates, A.J., Wahlund, J., 2009. Negative ion chemistry in Titan's upper atmosphere. Planet. Space. Sci. 57, 1558–1572. doi:10.1016/j.pss.2009.04.004.
Wahlund, J., Louarn, P., Chust, T., de Feraudy, H., Roux, A., Holback, B., Dovner, P., Holmgren, G., 1994. On ion acoustic turbulence and the nonlinear evolution of kinetic Alfvén waves in aurora. Geophys. Res. Lett. 21, 1831–1834. doi:10.1029/94GL01289.
Wahlund, J.-E., Boström, R., Gustafsson, G., Gurnett, D.A., Kurth, W.S., Pedersen, A., Averkamp, T.F., Hospodarsky, G.B., Persoon, A.M., Canu, P., Neubauer, F.M., Dougherty, M.K., Eriksson, A.I., Morooka, M.W., Gill, R., André, M., Eliasson, L., Müller-Wodarg, I., 2005. Cassini measurements of cold plasma in the ionosphere of Titan. Science 308, 986–989. doi:10.1126/science.1109807.
Wahlund, J.-E., Galand, M., Müller-Wodarg, I., Cui, J., Yelle, R.V., Crary, F.J., Mandt, K., Magee, B., Waite, J.H., Young, D.T., Coates, A.J., Garnier, P., Ågren, K., André, M., Eriksson, A.I., Cravens, T.E., Vuitton, V., Gurnett, D.A., Kurth, W.S., 2009. On the amount of heavy molecular ions in Titan's ionosphere. Planet. Space. Sci. 57, 1857–1865. doi:10.1016/j.pss.2009.07.014.
Waite, J.H., Niemann, H., Yelle, R.V., Kasprzak, W.T., Cravens, T.E., Luhmann, J.G., McNutt, R.L., Ip, W., Gell, D., De La Haye, V., Müller-Wordag, I., Magee, B., Borggren, N., Ledvina, S., Fletcher, G., Walter, E., Miller, R., Scherer, S., Thorpe, R., Xu, J., Block, B., Arnett, K., 2005. Ion neutral mass spectrometer results from the first flyby of Titan. Science 308, 982–986. doi:10.1126/science.1110652.
Waite, J.H., Young, D.T., Cravens, T.E., Coates, A.J., Crary, F.J., Magee, B., Westlake, J., 2007. The process of tholin formation in Titan's upper atmosphere. Science 316, 870–875. doi:10.1126/science.1139727.
Wei, H.Y., Russell, C.T., Wahlund, J., Dougherty, M.K., Bertucci, C., Modolo, R., Ma, Y.J., Neubauer, F.M., 2007. Cold ionospheric plasma in Titan's magnetotail. Geophys. Res. Lett. 34, L24S06. doi:10.1029/2007GL030701.
Whipple, E.C., Jr., 1965. The equilibrium electric potential of a body in the upper atmosphere and in interplanetary space. Ph.D. Thesis, The George Washington Univeristy.
Young, D.T., Berthelier, J.J., Blanc, M., Burch, J.L., Coates, A.J., Goldstein, R., Grande, M., Hill, T.W., Johnson, R.E., Kelha, V., McComas, D.J., Sittler, E.C., Svenes, K.R., Szegö, K., Tanskanen, P., Ahola, K., Anderson, D., Bakshi, S., Baragiola, R.A., Barraclough, B.L., Black, R.K., Bolton, S., Booker, T., Bowman, R., Casey, P., Crary, F.J., Delapp, D., Dirks, G., Eaker, N., Funsten, H., Furman, J.D., Gosling, J.T., Hannula, H., Holmlund, C., Huomo, H., Illiano, J.M., Jensen, P., Johnson, M.A., Linder, D.R., Luntama, T., Maurice, S., McCabe, K.P., Mursula, K., Narheim, B.T., Nordholt, J.E., Preece, A., Rudzki, J., Ruitberg, A., Smith, K., Szalai, S., Thomsen, M.F., Viherkanto, K., Vilppola, J., Vollmer, T., Wahl, T.E., Wüest, M., Ylikorpi, T., Zinsmeyer, C., 2004. Cassini Plasma Spectrometer investigation. Space Sci. Rev. 114, 1–112. doi:10.1007/s11214-004-1406-4.